# Studies of the Synthesis of SSZ-25 Zeolite in a “Mixed-Template” System

Stacey I. Zones,*[a] Son-Jong Hwang,[b] and Mark E. Davis[b]

**Abstract:** The synthesis of aluminosilicate zeolite, SSZ-25, is described using a two-component organic guest molecule strategy. This method has been recently described by us and is quite effective in crystallizing a variety of aluminosilicate zeolites with reduction in template cost. In this instance the original organic guest component used in the discovery of SSZ-25, *N*′,*N*′,*N*′-trimethyl-2-adamantammonium cation, is used in conjunction with a variety of smaller amines. The amine is the major organic component in the synthesis and the quaternary ammonium compound, while a minor component, is essential for structure direction to the desired zeolite product. Studies here show that the adamantyl component is preferentially taken up during crystal growth. Our studies showed that the use of the multi-organic component approach to synthesis resulted in a faster and cheaper route to crystallizing SSZ-25. The SSZ-25 has been described in the literature as having the MWW topology and as such has two different channel systems accessed by 10-ring openings; the channel systems do not intersect. One set of 10-rings open into large cavities. In this study we used NMR spectroscopy to examine the as-made materials and to see if the two organic components are used in different capacities in the synthesis, probing if the admantyl component is only found in these larger cavities. The crystalline products could be affected by solvent extraction with polar solvents like dimethylformamide; the X-ray powder patterns and elemental analyses changed with solvent treatment. The solvent-treated crystals were studied by NMR spectroscopy, elemental analysis, and argon adsorption. The two-component organic guest approach was also found to be quite flexible not only with regard to the amine, but also towards the quaternary ammonium compounds. Non-adamantyl polycyclic templates could be used, and polar but non-quaternized adamantyl derivatives also succeeded in directing towards SSZ-25 formation. On the other hand, in one instance it was shown that the two-component approach favors SSZ-25 as the kinetic product but at longer run times Ostwald ripening was observed, leading to the disappearance of SSZ-25 and formation of ferrierite zeolite and quartz.

**Keywords:** adamantane · amines · NMR spectroscopy · template synthesis · zeolites

## Introduction

Zeolite SSZ-25 is one of a series of materials reported in the literature as belonging to a topology described by the crystal structure assigned to the zeolite MWW.[1–5] SSZ-25 was the first description of the discovery of this material where a quaternary ammonium compound was used in the structure-directing function of the guest molecule to be found within the void spaces of the crystallized product.[6] Other reports utilized the cyclic amine hexamethyleneimine in the crystallizing of aluminosilicates PSH-3[7] and MCM-22[8] and piperidine for the borosilicate ERB-1.[9] These zeolite descriptions all pertain to the MWW structure, solved after all of the synthesis routes had been reported.[10] This topology is indeed one of the most complex and fascinating zeolite crystal structures described to date. Just the initial crystallization seems to produce an aluminosilicate structure whose bonding is not yet complete. Higher temperature treatments of the solid seem to produce the final bond-making,[11] generating a material with large cages accessed by 10-ring apertures and then a completely separate sinusoidal 10-ring channel sequence that winds its way around the large cavities, running perpendicular to the long dimension (18 Å) of the cages. A representation of the MWW zeolite and these features is given in Figure 1. With a high microporosity and such unusual structural features, it is not surprising that this material would have such an interesting and rich catalytic chemistry;[12–14] and a commercial application for the production of ethylbenzene has now been introduced.[15]

More recently Camblor and co-workers have made breakthroughs in the synthesis of all-silica materials, finding ways to make relatively low-density (highly porous) zeolites without extensive lattice substitution. Until their work, researchers generally experienced a trend where very high silica syntheses

---

[a] Dr. S. I. Zones
Chevron Research and Technology Company, P.O. Box 1627
Richmond, CA 94802 (USA)
Fax: (+1) 510-242-4647
E-mail: sizo@chevron.com

[b] Dr. S.-J. Hwang, Prof. M. E. Davis
California Institute of Technology
Department of Chemical Engineering, Pasadena, CA 92115 (USA)

0947-6539/01/0709-1990 $ 17.50+.50/0

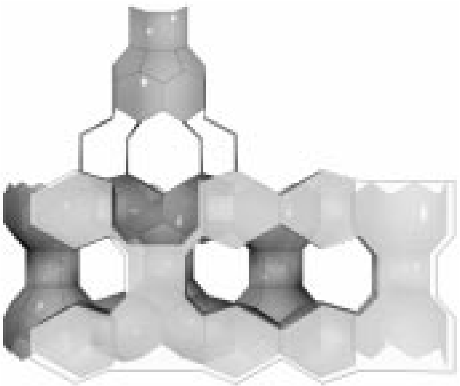

Figure 1. Representation of the MWW zeolite. One 10-ring system within the layer winds around the large cages but does not allow entrance into them. The large cavities are formed by connectivity from one layer to the next (our model shows just one), forming six adjacent 10-ring windows which circumscribe the center of the large cavity. The model was generated using FormZ and Electric Image software. We thank Kelly and Scott Harvey for their creativity in generating the image.

produced structures rich in 5-ring building blocks and containing relatively high framework densities.[16] Camblor and co-workers discovered the all-silica version of the MWW topology and termed it ITQ-1.[17] Their discovery utilized the same organo-cation, *N*,*N*,*N*-trimethyl-2 adamantammonium, which we had exploited in the initial discovery of SSZ-25 over a decade ago. Our initial exploration of the use of organo-cation derivatives was based simply on a desire to have a guest molecule too large to fit into ZSM-5. The zeolite literature in the 1980s had shown that a great many small amines and flexible polar molecules functioned well in crystallizing ZSM-5.[18] The success of our approach was that zeolites SSZ-13 (CHA), -23 (STT), -24 (AFI), and -25 (MWW) were all discovered. Inorganic components and their ratios often dictated which crystalline structure was produced.[19]

In 1998, Camblor's group, in collaboration with Baerlocher, published a comprehensive synthesis and structure study pertaining to ITQ-1 and related zeolites, many produced as mixtures in the studies with adamantyl quaternary ammonium compounds.[20] One of their more exciting results was the discovery that for all-silica, ITQ-1, the fastest crystallization rates (and sometimes better phase purity) were produced when a mixture of organic molecules was used. In their study they probe the prospect of different organic components performing the space-filling function of stabilizing the growing zeolite structure by virtue of unique residence areas within the structure for the different organics. Once the MWW structure had been revealed, it had been tempting to speculate that the larger adamantyl derivatives occupy the larger cages (as they do in the CHA structure, SSZ-13). So, the question arose as to what might be stabilizing the 10-ring sinusoidal regions.

This recent publication prompted us to expand upon similar results obtained for the aluminosilicate SSZ-25, described by one of us (SIZ) in a patent publication a few years ago. In that work,[21] we described a number of zeolite systems in which the structure-directing organo-cation could be used in very small amounts and larger amounts of small amines could be added as a second organic component with the successful crystallization of the desired zeolite. In the work we described for SSZ-25, two important discoveries emerged in addition to the success of the technique. As had been reported by Camblor and colleagues,[20] we had also observed a crystallization rate acceleration with the two organic component synthesis; but we also observed that the adamantyl component in the synthesis no longer had to be quaternary; both the simple amine and alcohol derivatives also produced SSZ-25 in the presence of additional polar amines.

In the present study we describe the additional data collected for the two-component synthesis of SSZ-25 as we have moved forward toward developing this approach for the catalytically active form of this zeolite (all-silicon has no acidic sites). As we were studying the aluminosilicate system, there was also an opportunity to compare how the two organic components may be able to function differently in this system as compared with the all-silica, ITQ-1, case.

## Results and Discussion

### Flexibility of the reaction

**Amines and templates**: Table 1 above gives some reactant ratios for the use of the two-organic approach to crystallizing SSZ-25. Table 2 has a matrix of two-component systems. In one set there is an adamantyl component. In the second set there is a supplementary component used in excess over the adamantyl derivative. The ratios are given in Table 1. Also, the intent was to use the adamantyl component at levels low enough that void filling during crystallization couldn't simply be accomplished by the adamantyl component alone. On the other hand, there is a necessity for the adamantyl component. Table 3 contains experiments aimed at clarifying the roles of amine, template and seeding in rapidly synthesizing SSZ-25. As can be seen in Table 3, where crystallization data for selected experiments is shown that for reactions carried out with seeding with SSZ-25, the two-component systems for isobutylamine or piperidine, coupled with smaller amounts of the *N*,*N*,*N*-trimethyl-2-adamantammonium cation (herein referred to as template B; see Table 2), produce a product faster than the template B alone. But, in the absence of the template, neither amine produces the correct product; piperidine yields ZSM-5 and is well known to be a good organic additive for ferrierite synthesis.[22] The free amine for adamantane, as well as the alcohol, also produced SSZ-25 when used in conjunction with a smaller amine. The use of the

Table 1. Ratios applied in typical inorganic synthesis (with $SiO_2$ as = 1).[a]

| | |
|---|---|
| $Al/SiO_2$ | 0.06[b] |
| $amine/SiO_2$ | 0.22 |
| $KOH/SiO_2$ | 0.20 |
| $H_2O/SiO_2$ | 44 |
| $adamantyl/SiO_2$ | 0.06 (or less) |

[a] Conditions: temperature 170 °C, RPM = 43. [b] Al source is Reheis F2000 aluminum hydroxide gel (dried, 53 wt% $Al_2O_3$).

Table 2. Matrix of comparative components.

| | | 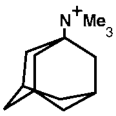<br>A | 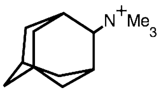<br>B | 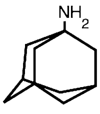<br>C | 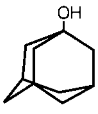<br>D |
|---|---|---|---|---|---|
| 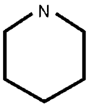 | 1 | × | × | × | × |
| 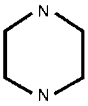 | 2 | | × | | |
| 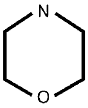 | 3 | | × | | |
| 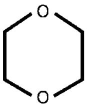 | 4 | | × | | |
| 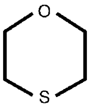 | 5 | | × | | |
| 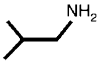 | 6 | × | × | × | |

Table 3. Crystallization rates for SSZ-25 using two organic components, with and without seeding (standard synthesis conditions are from Table 1 unless noted).

| Component 1 | Component 2 | Seeds | Days at temp. | Product XRD |
|---|---|---|---|---|
| piperidine | none | no | 6–7 | ZSM-5 |
| piperidine | B | no | 5–6 | SSZ-25 |
| piperidine | B | yes | 2–3 | SSZ-25 |
| cyclopentylamine | none | no | 5–6 | ZSM-5 |
| cyclopentylamine | B | yes | 3–4 | SSZ-25 |
| isobutylamine | none | no | 7–10 | SSZ-32 (Al-rich MTT) |
| isobutylamine | B | yes | 2–3 | SSZ-25 |
| isobutylamine | B[a] | no | 4–5 | SSZ-25 |
| isobutylamine | B[b] | no | 6 | SSZ-25 |
| none | B | no | 10 | SSZ-25 |
| none | B | yes | 6 | SSZ-25 |

[a] $B/SiO_2 = 0.10$. [b] $B/SiO_2 = 0.20$.

hydrocarbon adamantane was not successful; and one difficulty observed was that it had virtually no solubility in the reaction system, floating on top as nice crystals. The polar derivatives have a chance to be solvated in these high ionic-strength aqueous systems. Reactions proceed more rapidly in the presence of seeds.

**Use of heterocyclic compounds and templates**: The reaction was also carried out with other heterocycles with space-filling comparable to piperidine. The series of two-component systems is indicated in Table 2. Each reaction involving template B and a heterocycle was run for 1–4 days with a reactor dedicated to each time point. Typically, the crystallization kinetics of a given reaction were analyzed by X-ray diffraction measurements, where the progress, relative to a 100% crystalline standard, can be proportionally measured. But for crystallizing zeolite materials with X-ray diffraction (XRD) patterns with broad lines (and recall that the MWW crystal is not considered even completely formed at this stage), the value of comparing amplitudes of certain peaks within the patterns may not be the best measure of extent of crystallization. Instead, we took the as-made samples, calcined them, and then analyzed for the available nitrogen micropore volumes, as reflected in the surface areas measured. Using this approach, we established that the system with piperidine as the amine component gives superior product crystallization over the other heterocycles (Table 4). The optimum value achieved is also the same as the SSZ-25 material made with template B as the only component. The XRD data had indicated that the piperidine-based system looked finished after two days at crystallization under these conditions. The micropore experiments suggest that the product was improved by heating for a third day. For the isobutylamine route to SSZ-25, we find that the zeolite produced by that method also gave a very high micropore volume after calcination. This indicates that the amine functionality may be more important in successful crystallization (and possibly pore-filling) than polarity based upon oxygen or sulfur as in dioxane and thiomorpholine. The latter two molecules gave the poorest SSZ-25 product based upon micropore values at a certain time of crystallization. It is surprising that the more basic compounds like piperazine and morpholine were not as effective as piperidine.

Table 4. Micropore volumes for calcined SSZ-25 samples.

| Code for route (Table 2) | Surface area [$m^2 g^{-1}$] |
|---|---|
| B1 | 460 |
| B2 | 296 |
| B3 | 200 |
| B4 | 274 |
| B5 | 210 |
| B6 | 500 |
| B alone | 500 |
| C6 | 500 |

**Structural changes brought about by solvent treatment**

An unusual feature of the synthesis of SSZ-25 is that a relatively dramatic change in XRD scattering angles can be observed in comparing the as-made and calcined SSZ-25. Previous published work on the MWW structure discussed the possibility that the zeolite structure was actually not complete in the as-made form. Calcination was described as completing some bond formation, and a contraction of the *c* axis of the unit cell was observed.[11] We were surprised to find that this structural shift could be mimicked by solvent treatment of the as-made material, at a temperature well below the decomposition temperatures seen for the template during calcination (onset near 300 °C from thermogravimetic analysis mass spectrometric (TGA MS) studies). A good example of the solvent treatment is to heat the as-made zeolite in an excess of dimethylformamide near the boiling point (150 °C). Figure 2

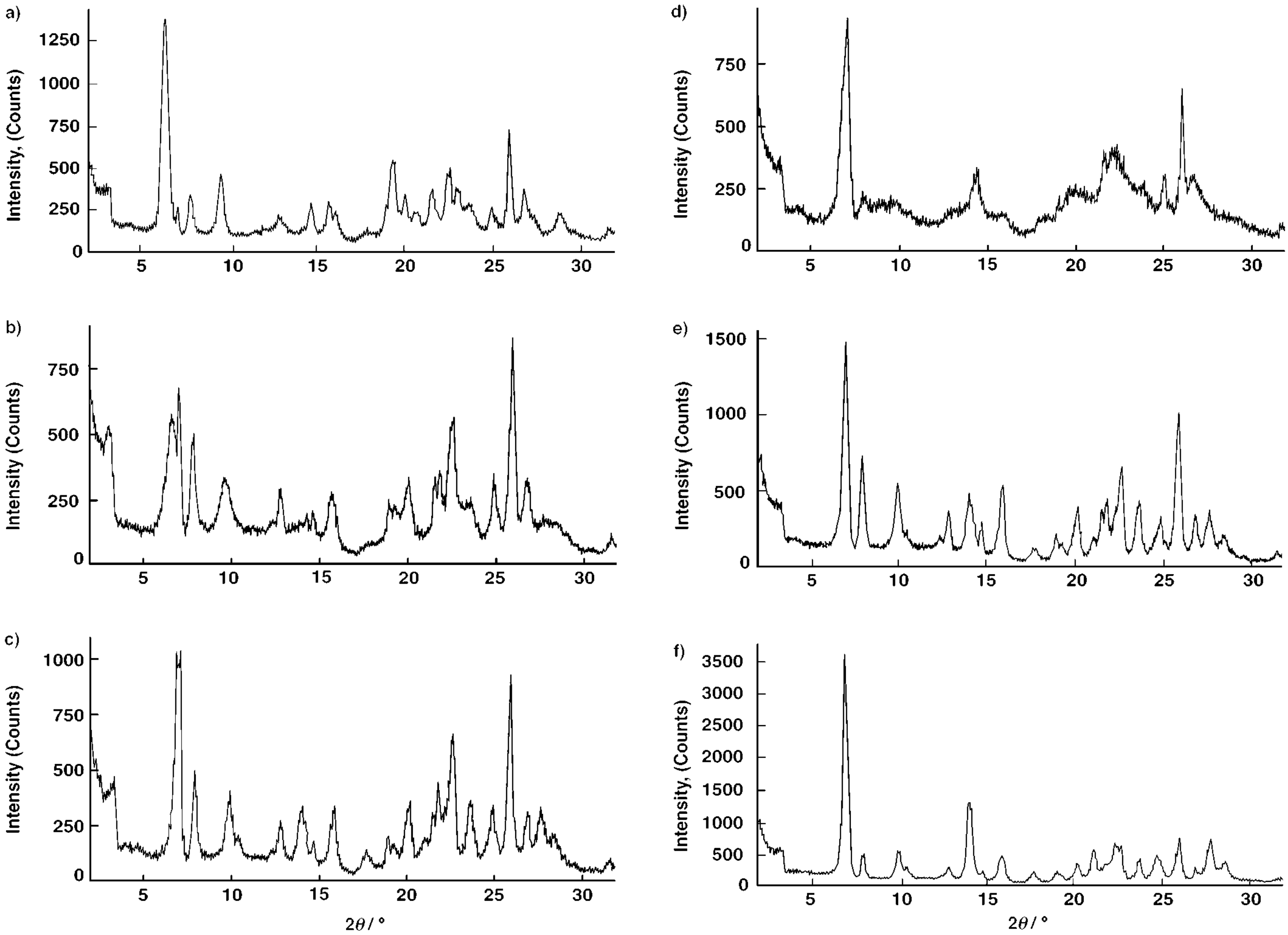

Figure 2. Comparative XRD patterns for SSZ-25 samples. Patterns a), b), and c) are for as-made materials using only template, then the mixed system with decreasing template (run code B6(a)–(c), respectively; see Tables 6 and 7 for more detail). Patterns d), e), and f) are the corresponding patterns for the materials after they have been treated with DMF.

shows the XRD patterns before and after treatment for the material in code slot B6 (see Table 2), where two different ratios for B6 were used in the synthesis. The shift upon treatment gives a pattern much like that of the calcined material (Figure 2d–f). Organic material is removed from the solid during the treatment. The C,H,N data for two different SSZ-25 materials (B6 and C6; see Table 2), before and after the treatment is given in Table 5. We also show the changes for the SSZ-25 made from just template B. While there is substantial reduction in hydrocarbon content, we do not believe that this comes from out of the zeolite pores alone. The data for the SSZ-25, formed from B alone, indicates that a) the treatment can reduce the organic content by a third and that b) the adamantyl component, which is B, is too large to remove from the pores and shows no propensity to decompose at a temperature as low as 150 °C. A possible interpretation is that there is also organic material between sheets of the SSZ-25 crystals. As has been much discussed in the recent zeolite literature, the MWW material crystallizes with a thickness of a relatively few unit cells.[23] A recent report from the Corma Group described delamination approaches (as one might use with a clay) resulting in nearly single-layer sheets of MWW; this material, with differences in catalytic performance over the normal MWW, was termed ITQ-2.[23]

Table 5. Changes in organic content after DMF treatment.

| System | As made [wt %] | | | After DMF [wt %] | | |
|---|---|---|---|---|---|---|
| | C | H | N | C | H | N |
| B alone | 10.55 | 1.91 | 1.02 | 7.49 | 1.42 | 1.05 |
| B6(a) | 11.79 | 2.02 | 1.53 | 9.60 | 1.72 | 1.27 |
| C6(b) | 7.48 | 1.52 | 1.20 | 7.24 | 1.35 | 1.27 |

The highest total organic content found in the crystalline SSZ-25 products was 15 wt%. The available micropore volume for this structure is about 0.18 cc$g^{-1}$ for nitrogen. Based upon coking studies we have carried out, we estimate that approximately two-thirds of the micropore volume resides in the large cavities. At a micropore volume then of roughly 0.12 cc$g^{-1}$, this would be a value similar to the large pore zeolite SSZ-24 also specified in its synthesis by a quaternized adamantyl compound. There the organic/$TO_2$ ratio needed to fill the pore system is about 0.04. This also translates into about 12 wt% of the as-made product, and this is observed for the crystallized product. Thus the large cavities of SSZ-25 should be filled at a adamantyl quaternary/$TO_2$ ratio of about 0.027 (0.04 × 2/3). The question then remains as to whether any of the adamantyl derivative also sits in the incompletely formed cavities which make up the sheet surfaces.[23] This could explain the loss of organic material when dimethylformamide treatment is carried out on materials which were synthesized in the presence of only quaternized adamantyl component.

### Experiments in the light of two independent channel systems

**Adamantyl components**: The point has been made that the MWW structure contains two entirely different micropore systems. Each is accessible by 10-ring openings; but in one case, the 10-rings open into cavities bounded by 12-rings and running 18 Å in length.[11] We are interested in whether the two organic components used in these new syntheses play different roles in stabilizing the two independent channel systems. It can be assumed that the adamantyl component only fits into the larger cages; the other sinusoidal 10-ring system does not appear to have a region large enough to accommodate the polycyclic component with a "girth" of greater than 6.2 Å. The majority of the work considered will deal with template B rather than A.

Figure 3 gives an indication that template B is much more stable to decomposition under the basic pH of the reaction medium. (Hofmann Degradation is the expected competing reaction for the fate of the template.) To probe the fate (and use) of organic molecules in this two-component system, a comparison was made for the use of isobutylamine at constant concentration, contrasted with variable amounts of adamantyl component in the synthesis. The fixed amine quantity was always in molar excess over the adamantyl component. The systems with quaternized $Me_3N^+$-adamantammonium (B) and the free 1-amine (C) were examined. The ratios employed and the XRD data are given in Table 6. The runs are coded as B6(a)–(c) and C6(a)–(c). One of the surprising results was that at high 1-adamantanamine concentrations, the clathrasil, Sigma-2, was formed.[24] Figure 4 shows that the round cage can easily accommodate such a guest molecule. Each of the materials recovered from the zeolite syntheses described in Table 6 was split into two parts. The first was analyzed for C, H, and N and then analyzed by $^{13}C$ MAS NMR spectroscopy. The second portion of each run was treated with DMF, then filtered , washed, and dried. The representative XRD data was obtained. Then, these treated samples were analyzed for C, H, and N, content, and also studied by $^{13}C$ MAS NMR spectroscopy. The before-and-after treatment C, H, and N data are given in Table 7.

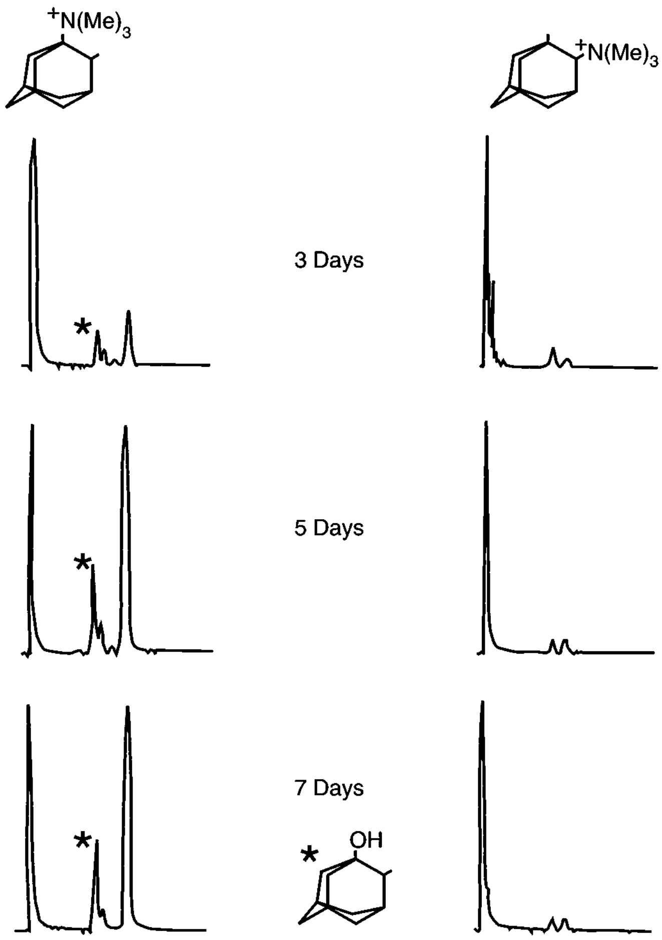

Figure 3. Decomposition of organo-cations during the SSZ-25 synthesis at 175 °C. We made two comparative GC runs of ether extracts of the zeolite synthesis run for SSZ-25. The traces show that the adamantyl derivative substituted at position 1 gives more Hofmann degradation product than the structure-directing agent (SDA) with substitution at position 2. The decomposition is also seen to increase with time in the case of the first isomer. The presence of the product adamantyl alcohol was determined by chromatography.

Table 6. Parameters for synthesis runs using isobutylamine and the larger adamantyl component.

| Run code | $i$C$_4$NH$_2$ [mM][a] | B [mM][a] | C [mM][a] | Product |
|---|---|---|---|---|
| B6(a) | 3 | 1.5 | 0 | SSZ-25 |
| B6(b) | 3 | 0.75 | 0 | SSZ-25 |
| B6(c) | 3 | 0.38 | 0 | SSZ-25 |
| C6(a) | 3 | 0 | 1.67 | SIGMA-2 |
| C6(b) | 3 | 0 | 0.67 | SSZ-25 |
| C6(c) | 3 | 0 | 0.33 | SSZ-25 |
| B alone | 0 | 3.0 | 0 | SSZ-25 |

[a] Relative to 15 mM of $SiO_2$ in the synthesis.

The DMF treatment shows that material has been removed from the as-made zeolites. The change is not uniform. As expected, the clathrasil, Sigma-2, shows very little change. The organic is trapped in the cages of the clathrasil, and this solvent treatment doesn't really remove these guest molecules. The effects are more dramatic for the SSZ-25 samples. Within this series, the most pronounced change is occurring for the carbon content for the B6 series. As the amount of B available in the synthesis is reduced, the SSZ-25 is still crystallized; but there is a larger difference in the carbon contents before and after this solvent reflux treatment. This could suggest that it is mainly isobutylamine being removed at this stage. With isobutylamine, unlike the discussion about adamantyl components given above, it could be possible that it is being removed from the pores by the treatment. A further indication of the removal of isobutylamine from the pores is also found from examining the shift in intensity for certain low-angle peaks. A very general phenomenon in high silica

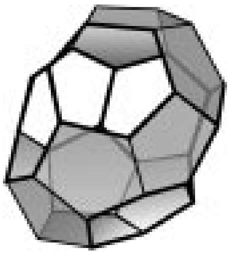

Figure 4. Model of the larger and unsymmetric cage in Sigma-2. The cage is composed of 5- and 6-rings and contains the adamantamine molecule. A comparison with Figure 1 suggests that the large cavity in SSZ-25 is more than twice as large. One question that arises is whether there are two admantamines per large cavity in the synthesis with this template.

zeolite chemistry is to have XRD patterns experience large intensity changes for low-angle peaks after calcination. This has been attributed to removal of guest molecules from the pores. Figure 5 shows comparative XRD patterns for the two-component SSZ-25 synthesis but also from the B only system. In the latter, the DMF treatment does shift the diffraction angles, as we have seen for other systems. But, a comparison of peak intensity at $2\theta = 7.0$ shows not much change for the material made from an adamantyl component only; it cannot be removed from the pores by solvent treatment. Conversely, the sample with a high ratio of isobutylamine to B shows no *d*-spacing shift, but a dramatic change in intensity after DMF treatment. That isobutylamine is removed from the zeolite by DMF treatment was also verified by NMR studies (vide infra).

Table 7. Carbon, hydrogen, and nitrogen analyses [wt %] for as-made and DMF-treated zeolite samples.

| Run code | As-made | | | DMF | | |
|---|---|---|---|---|---|---|
| | C | H | N | C | H | N |
| $C_6$(a) | 9.79 | 1.45 | 1.12 | 10.05 | 1.48 | 1.26 |
| $C_6$(b) | 7.48 | 1.52 | 1.20 | 7.24 | 1.35 | 1.27 |
| $B_6$(a) | 11.79 | 2.02 | 1.53 | 9.60 | 1.72 | 1.27 |
| $B_6$(b) | 10.70 | 1.91 | 1.55 | 6.69 | 1.17 | 1.41 |
| $B_6$(c) | 9.35 | 1.78 | 1.40 | 5.66 | 1.19 | 1.17 |
| B alone | 10.55 | 1.91 | 1.02 | 7.49 | 1.42 | 1.05 |

**Magic angle spinning $^{13}$C NMR analysis of solids**: Figure 6 shows $^{13}$C MAS NMR spectra. Template B in the iodide form and in the solid state is shown as a reference spectrum. Likewise, the hydrochloride salts of isobutylamine and adamantamine are given. Figure 7d shows the spectra for template B alone as the organic system in the synthesis of SSZ-25. With these spectra as reference points, one can begin to analyze the $^{13}$C MAS NMR spectra for the crystallized materials in the series B6 and C6. Figure 7 shows a comparison of the crystallization product, Sigma-2(Figure 7a), the SSZ-25 product from a mix of isobutylamine and 1-adamantanamine (template C; Figure 7b), and then the product in Figure 7b after DMF treatment (Figure 7c). Nicely shown by absences is the fact that the Sigma-2 can form without using isobutylamine. The isobutylamine used in a successful synthesis of SSZ-25 with C does remain in the product, but the DMF treatment removes isobutylamine and C remains in the product.

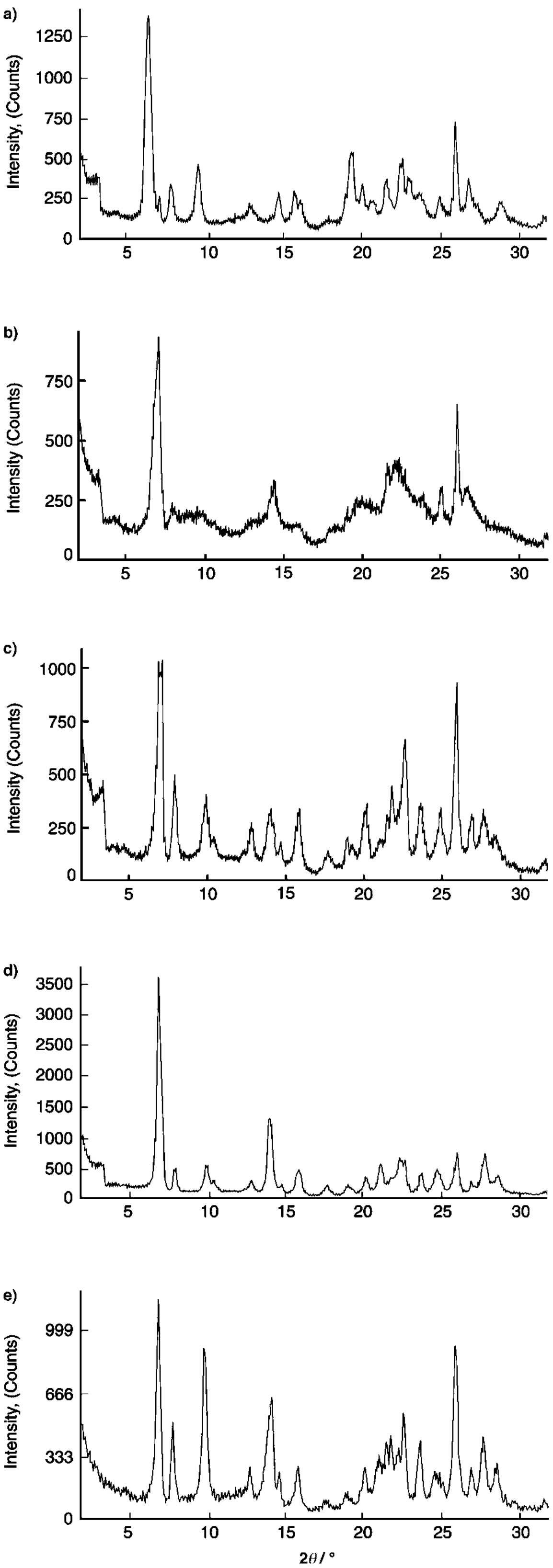

Figure 5. Comparison of the XRD patterns for SSZ-25 a) made with B alone and b) made in a mixed SDA system. c) XRD pattern for the DMF treated material from a). d) XRD pattern for the DMF treated material from a mixed SDA run. e) XRD pattern for the calcined material from a). After DMF treatment of each, it can be seen that the intensity increases much more dramatically in the mixed SDA system. For B alone, the peak positions shift but without too much change in intensity (unless the organic component is completely removed by calcination).

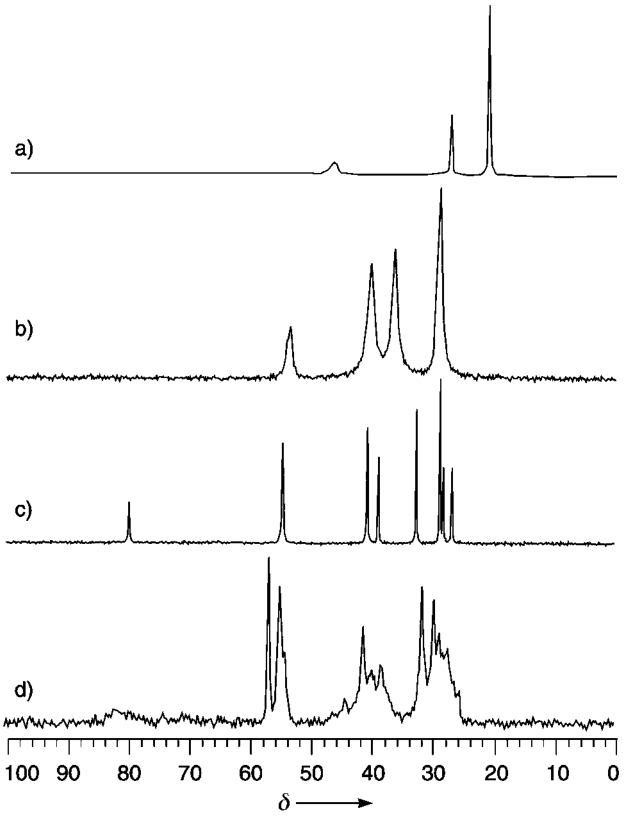

Figure 6. Reference $^{13}C$ MAS NMR spectra. a) The quaternized isobutylamine in the solid state. b) The quaternized adamantamine in the solid state. c) The quaternized template B in the solid state. d) The MAS NMR spectrum of SSZ-25 from template B alone.

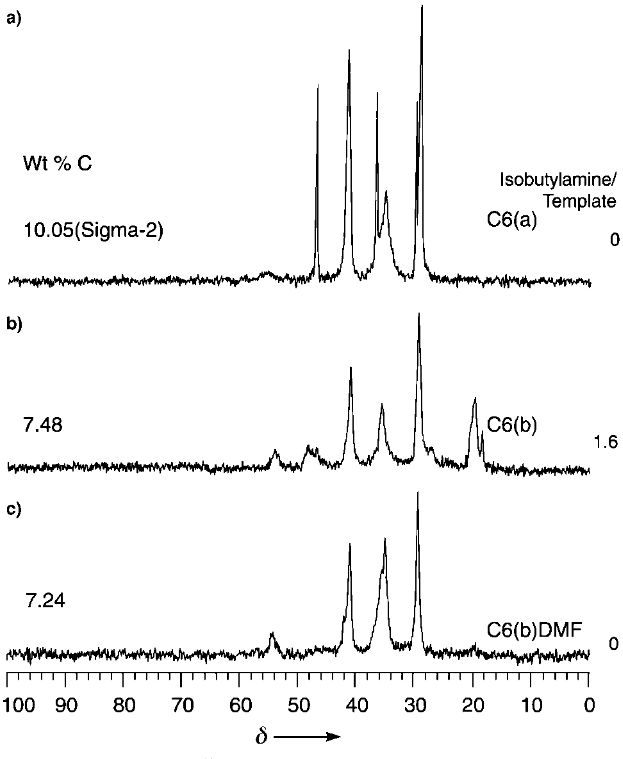

Figure 7. Comparative $^{13}C$ MAS NMR spectra for SSZ-25 samples. a) Spectrum for the sigma-2 product formed; b) spectrum for the mixed SDA system; c) spectrum for the DMF treated material in b). No change occurs for the DMF treated material from a).

Figure 8 shows a series of comparative spectra for three zeolite runs producing SSZ-25 in the B series and then the spectra after DMF treatment. Also shown in the figure are the ratios of each pore-filling component as determined by NMR spectroscopy. It can be seen in rather spectacular fashion, that isobutylamine, present in cationic form in the zeolite, is being removed from the SSZ-25 by the treatment. This is also reflected by the reversal of component ratios as measured by NMR spectoscopy and shown in the margins. Notably, the contribution by isobutylamine is greatest in the product in which the least adamantyl derivative is supplied to the synthesis. This secondary amine component appears in the crystalline product but can also be removed to a sizable extent by the solvent DMF treatment. The zeolite synthesis occurs in a pH range of 11–12, above the $pK_a$ for these amines. But even at these pH values the equilibrium expression $K_a$ would show a minor amount of protonated amine. This latter component may be preferentially sequestered into the growing zeolite.

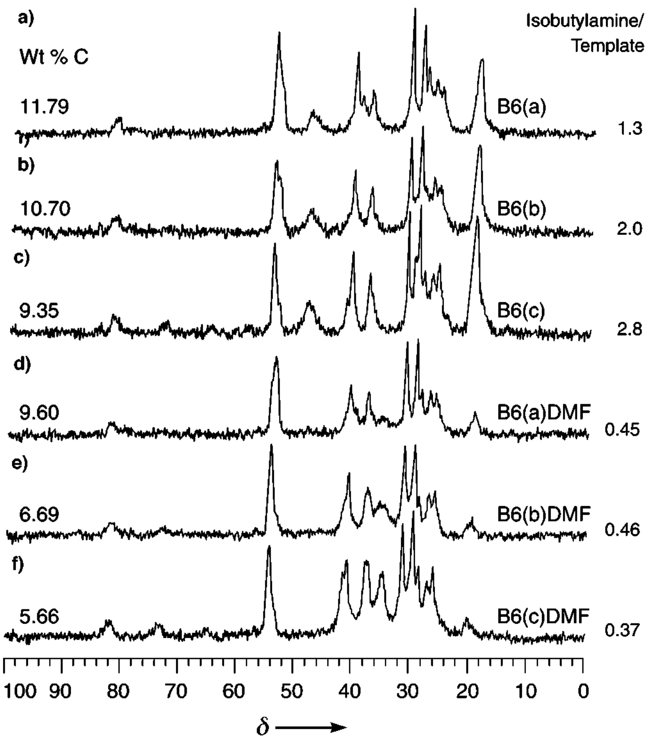

Figure 8. $^{13}C$ MAS NMR spectra for samples in the B6 series recorded for various ratios of adamantamine to isobutylamine. Numbers in right margin are for the NMR ratio of isobutylamine to template B. a)–c) Show the increasing contribution of isobutylamine in the product. d)–f) Show how DMF has removed isobutylamine from these samples, even though it is recognized as being in the quaternized state.

There are two independent measurements of template use. We can attempt to deconvolute the two organo-cation contributions from the C, H, and N elemental analysis data or we can attempt to directly quantify the situation from the NMR spectra. In Figure 9 we have plotted the two measurements against each other to see if there is a correlation even if complete agreement is not found. Then the values are plotted against the reactant ratios (Figure 10). In this latter instance, it becomes easier to see that the adamantyl derivative is

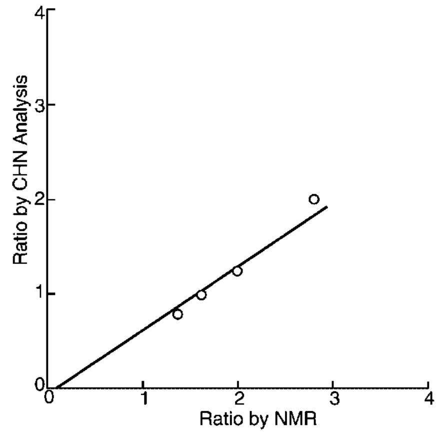

Figure 9. Plot of a comparison of the two components in the product from either NMR analysis or deconvolution of the elemental analysis. While the two methods are linearly correlated, they do not produce the same absolute values.

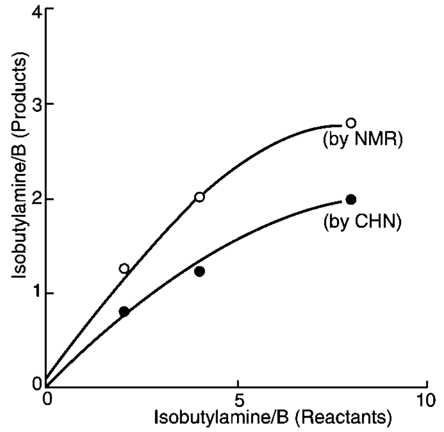

Figure 10. Plot of the results of the analyses from Figure 9 against the reactant ratios in SSZ-25 synthesis experiments. This shows that the adamantyl components are preferentially incorporated in the synthesis.

preferentially incorporated into the final, crystallized product. This is sensible from the standpoint that the most important necessity may be the stabilization of the large, open cavity. This point is worth making given that the inorganic parameters being explored (most notably SAR, or silica-to-alumina ratio, =35) lend themselves well to the crystallization of either ZSM-5 (MFI) or ferrierite (FER) without the use of an organo-cation guest at all.[25, 26] The danger of this consequence is that the MWW product has the most open void regions of the three, and without stabilization, should subsequently recrystallize to the more dense phases in accord with the concept of Ostwald ripening.[27]

**Other templates**: The formation of this phase does exhibit a flexibility within the context of the synergism of polycyclic guest molecules and a relatively narrow range of inorganic reactant parameters. With isobutylamine in 5–10 fold excess over the polycyclic component, we have found other successful guests outside the boundaries of the adamantyl group (Table 2) for inducing the nucleation and crystallization of this zeolite phase. Scheme 1 depicts a range of structures, many of which have been used successfully to make other zeolites once set in different synthesis contexts. A number of them have been found to produce the more recently discovered, cage-based zeolites, SSZ-35 and 36.[28, 29] Once again we assume that these polycyclic templates stabilize the large cavities.

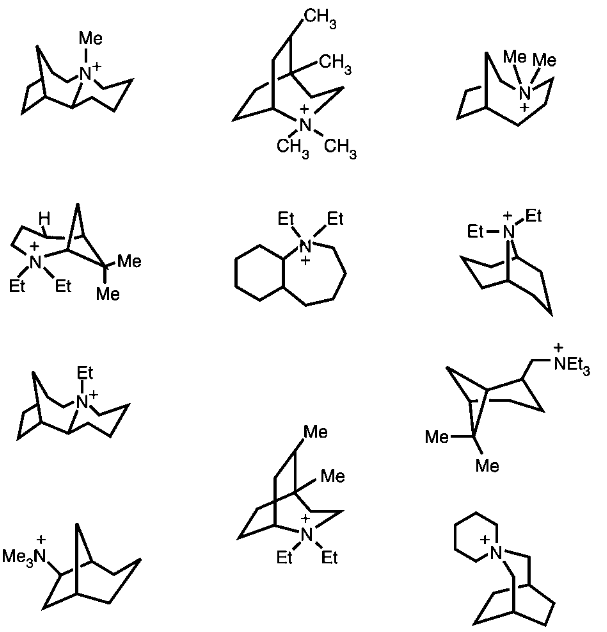

Scheme 1. Other organo-cations capable of crystallizing SSZ-25 when used with isobutylamine.

## Discussion of MWW growth formation

**Stabilizing two different channel systems**: The discovery, development, and subsequent follow-up towards commercial use of the MWW zeolite structure largely focused on materials with SAR in the range of 20–40. In earlier synthesis reports it appeared that a high silica version might be difficult to obtain, the incorporation of aluminum atoms into parts of the framework being possibly a critical parameter. In that light, it was a remarkable achievement for the group of Camblor, Corma, and co-workers to find a synthesis route leading to the all-silica ITQ-1. They once again demonstrated they had found a breakthrough route to crystallize relatively low density zeolites as all-silica products.[30] This went against the known trends.

In their recent discussion concerning ITQ-1 crystallization, they also described advantages for a two-organic-component approach for zeolite synthesis. They made a point that both types of channel system need stabilization in these essentially all-silica syntheses—we agree. There is very little precedence for high silica materials, with void regions that are not stabilized by guest molecules. Even the notion that water could fulfill such a role does not seem to be well supported in the literature. There are reports of clathrasil cages being stabilized by nonpolar adsorbates where the guest molecule seems to have a less specific function.[31]

Thus, one of the difficulties encountered in the all-silica synthesis using only adamantyl derivatives like template A was that the reactions required long periods of time. There was speculation that the secondary channel system could be filled by decomposition products from template A. We have shown in Figure 3 that template A does give more decomposition than template B, the latter showing very little tendency; but our data shows a principal decomposition product of the adamantanol coming from template A. This suggests that a by-product would likely be trimethylamine. Thus, the introduction of second amine components like hexamethyleneimine and dipropylamine made the synthesis of the all-silica ITQ-1 both faster and more reproducible.

In the aluminosilicate case, the issues may be different. In our early discovery of SSZ-25, only template B was used. The elemental analyses (see also Table 5 here) indicated that the trapped organic material was compositionally fairly close to template B. If there was decomposition leading to stabilization of the secondary pore system it was not in proportion to the void volume of this latter system. Crystallizing in a range of SAR = 25 – 40, the inorganic chemistry is also very much in the range of conditions for the synthesis of ZSM-5 (MFI) without any organic guest component.[32] In fact, it has been shown that even this range can be extended in the case of using sodium cations in the crystallization of ZSM-5.[33] Lowe and co-workers observed the same success for ZSM-5 in the potassium-based inorganic synthesis.[34] It is possible that hydrated alkali cations, counterbalancing aluminate centers present with some frequency in the structure, may be carrying out such a void stabilization role. In the crystallization of SSZ-25 from template B, it may also be the case that inorganic cations stabilize the smaller, secondary system. We have brought forth good evidence that the adamantyl components should not be found in this second channel system. The fact that the synthesis progresses much more rapidly (over template B alone) when the amount of template is reduced and a second component is introduced into the gel may indicate that an organic guest molecule may stabilize the second channel system much more effectively through nucleation and initial crystal growth.

**Template selectivity**: While the discovery of this two-component system comes with many benefits, like faster crystallization rate, greater template flexibility, and better economics based upon using much lower amounts of the more expensive template, there is evidence that the structure-direction function is not as exacting. In a paper by Davis and Lobo, the authors stipulated that to obtain a true templating effect, the organic guest component must only be capable of producing that single zeolite structure. At that time, the only example they cited was ZSM-18.[35] Because the zeolite crystallization reaction is often considered an example of Ostwald ripening and the products isolated by the researcher are generally metastable relative to other phases which could be formed from the same components, the "true" template effect has some advantages. To generate only a single, given structure, the fit in the zeolite void regions must be very tight and energetically favorable.[36] This will mean that the rate of dissolution will be very slow. It also means that if some template is available in solution, it is not very likely to nucleate yet another zeolite phase. That the latter could grow at the expense of the former over time is a good example of kinetic versus thermodynamic product selectivity where a given organo-cation is less selective. Because our combined molecule approach, even if each occupies a different spatial niche, does not seem to show as much selectivity, there will be less product stability through time. In fact, we find that after 10 – 12 days at a temperature of 170 °C, for the combined piperidine – template B system, the SSZ-25 disappears and ferrierite (FER) is now the product. We were actually able to sample over time from an 0.6-liter reactor and watch the SSZ-25 set of peaks early in the reaction and then see them decay as FER grew. The change in product over time is shown in Figure 11. One can also see the appearance of some quartz. In the Ostwald ripening process here, there may be some disproportionation of the T-atom components. The ferrierite, whose form may be more Al-rich than the parent SSZ-25, grows, leaving additional silicate to subsequently crystallize as the dense product, quartz. We were also able to mimic this result at constant synthesis time by running a series of reactions, each with increasing KOH concentration. As $OH/SiO_2$ is raised in the syntheses, the product increasingly is ferrierite with eventually, no SSZ-25 seen.

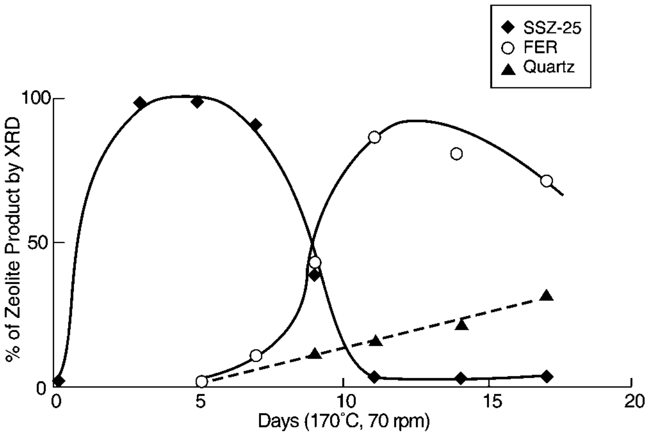

Figure 11. Plot of the crystallization versus time indicates Ostwald ripening. SSZ-25 is formed first, to eventually be replaced by the denser products, ferrierite and quartz. It may well be that a disproportionate use of T-atom components occurs in this subsequent transformation, with ferrierite becoming Al-rich over SSZ-25 and quartz constituted as mostly silicate.

This result is consistent with an observation made for the MCM-22 crystallization system that uses hexamethyleneimine. Mochida and colleagues showed that FER had already formed at the end of one week of crystallization and was even more favorable in syntheses that were started near the more Al-rich boundary for MCM-22 formation.[37] Here was a case where the same organic amine could stabilize either structure. The more open framework formed first and then was replaced by the denser zeolite product.

Our experiments with different adamantyl derivatives (Table 2) have already demonstrated that the molecules used in filling the large cavities or cages in MWW materials do not have to do so with great specificity. The assumption here is that none of the adamantyl derivatives is found in the other

10-ring system. Further verification for the flexibility of this feature comes from the fact that a variety of polycyclic molecules, used in conjunction with isobutylamine, produce SSZ-25 even when that was not the intent. The reactions were carried out without seeding but using the ratios given in Table 1. Often, crystallization took much longer than the few days shown in the optimal reactions with adamantyl derivatives. The product was often found after 1–2 weeks of heating. From the recrystallization sequence discussed above involving piperidine and FER formation, it is also clear that running a reaction for one week or more, in the presence of isobutylamine, is clearly much less risky in terms of Ostwald ripening. Scheme 1 depicts a number of other polycyclic structures that successfully crystallized SSZ-25. Again, what they have in common is a molecular width preventing them from fitting into a 10-ring channel and the presence of a charged, quaternary ammonium compound. All are polycyclic hydrocarbon skeletons. It is quite possible that for some of these molecules, even the basic amine functionality, prior to quaternization, may have successfully worked given our experience with adamantanamine.

**Relative micropore contributions for two-channel systems**: In preparation for determining the guest chemistry in the formation of SSZ-25 (because the microporous systems have been described as independent), it might be possible to assess how much of the void space resides in the larger cavities and then in the sinusoidal channel system. We can see the influence of both systems in the argon uptake data. Even though both windows of access to the two systems are 10-ring, one can guess that they are not equivalent. Molecules like cyclohexane are not adsorbed to the same extent as *n*-hexane or the gas molecules nitrogen and argon.[38] Presumably, cyclohexane is only working its way into the larger cavities. There will be more room for molecules to "turn the corner" in going through the 10-rings which access the large cavities that have internal 12-ring diameters. Because we have carried out SSZ-25 syntheses with different relative contributions of adamantane derivatives, these compounds might show differential uptake in the as-made, zeolite product. An analysis was carried out on the samples in the B6 series (see Table 6) and the template B alone. After performing the DMF treatment on the samples (NMR data had shown that some amount of isobutylamine is removed in this treatment) the samples were next evacuated to 7 millitorr for 24 h, while being heated to about 80 °C. Next, the samples were dried to 150 °C before being evaluated for argon uptake. We found no trend related to the amount of template B used in the synthesis, and the uptakes were remarkably low compared to those for the calcined material. Values were typically 0.02–0.03 cc$\,g^{-1}$ and instead of observing a bimodal uptake at two different filling pressures, there was simply a broad, intermediate filling point. These experiments suggest that there was not a simple demarcation of pores of one type being blocked and pores of another type being open in the DMF-treated SSZ-25. The data must also still give a little pause concerning the concept that the adamantyl derivatives are not at all to be found in the sinusoidal pore system. Clearly there seems to be at least a little partial blockage of this system from the argon data. It remains undetermined whether this blockage is due to adamantyl components, to some remaining isobutylamine cations, or due to even residual potassium cations.

## Conclusion

We have shown that a two-component organic additive system has a great flexibility in crystallizing the aluminosilicate, SSZ-25. Large polycyclic hydrocarbon quaternary ammonium cations most likely occupy the larger cages in the structure. In our work the two-component system shows faster crystallization rates over use of the polycyclic component alone. For secondary organic additives, amines worked better than heterocycles containing other polar atoms. The enhanced crystallization rate result was also seen in the work by Camblor and co-workers concerning the synthesis of the all-silica ITQ-1 having the same MWW topology as the SSZ-25.

As the amount of polycyclic quaternary ammonium compound is reduced in the synthesis mixture, a larger amount of the secondary amine component (isobutylamine in many of our studies described here) was found in the crystallized product. This was seen by NMR studies on the as-made products. NMR spectroscopy also showed the secondary amine to be present in a quaternized state. Yet reflux of as-made product in dimethylformamide seemed to indicate that isobutylamine could be removed; the site left behind must be balanced by a proton at this stage.

The XRD patterns of the as-made SSZ-25 products are also altered by the reflux treatment with dimethylformamide solvent. The patterns begin to look like those materials which have been calcined. But in fact the materials have been only treated to 150 °C. The fact that a sample with much lower polycyclic quaternary ammonium content (sample B6c) shows less shift in low angle, $2\theta$ peaks in the XRD pattern, indicates that the polycyclic quaternary ammonium compound normally has a role in crystallizing a product with material possibly residing in incomplete cavities between sheet layers of the crystalline product. This arrangement has been described by Corma et al.,[23] and the overall crystalline structure is incompletely bonded at this stage. On the other hand, samples with the lowest initial polycyclic quaternary ammonium compound available in the synthesis mixture also gave crystalline products, which after dimethylformamide reflux gave the greatest peak intensity changes at low angles of $2\theta$. This means a greater amount of material could be removed from the pore system, chiefly being isobutylamine.

Comparative studies by NMR spectroscopy and then by elemental analyses show that the adamantyl compounds (as examples of polycyclic quaternary ammonium components) are preferentially taken up in the synthesis of the growing crystalline product. This occurs even when the other organic component, isobutylamine, is present in much larger concentration. The adamantyl compound is needed to specify which zeolite will crystallize. On the other hand, the specification is loose enough that Ostwald ripening can eventually transform the crystallized SSZ-25 to other products. In a study using an adamantyl compound and piperidine, SSZ-25 was the initial product, eventually giving way to the production of ferrierite and quartz as the heating was continued past the point of the initial SSZ-25 production.

The aluminosilicate SSZ-25 can probably grow without the secondary pore system being filled with an organic component. This is likely to be the case when only a quaternized adamantyl derivative is used. Hydrated alkali cations, associated with aluminate framework sites, may fulfill this function. In the all-silica regime of crystallizing ITQ-1, this is less likely to be the case. The longer synthesis times may provide opportunities for the degradation products from the initial quaternized, adamantyl component to supply the smaller components to fill the secondary pore system. There is not much precedence in the literature of water performing this function in all-silica products.

## Experimental Section

**Synthesis**: The synthesis of the *N,N,N*-trimethyl-2 adamantyl ammonium hydroxide template has been described in the original patent. In general terms, this organo-cation is made in two steps. Starting with commercial 2-adamantanone, this molecule is heated in a closed system to near 175 °C with formic acid and dimethylformamide (Leuckhart Reaction), transforming the keto functionality to a dimethylamino derivative. Upon extraction (into diethyl ether) of this component from a basic aqueous solution during the reaction work-up, the product dimethylamino oil was isolated from diethyl ether, which had been dried with sodium sulfate. One equivalent of methyl iodide was used to quaternize this product (a variety of moderately polar solvents work), and the organo-cation was prepared as the hydroxide compound by exchanging the iodide form of the cation over an AG 1-X8 (BioRad) resin.

Zeolite syntheses were carried out using a combination of organo-cation hydroxide and a second amine component. In some instances, the quaternary ammonium compound was replaced by neutral adamantyl derivatives. Aluminate was supplied as Reheis F-2000, a dried aluminum hydroxide gel (53–56 wt% $Al_2O_3$). KOH was used as an alkali source, and Cabosil M 5 was used as the silica source. The secondary component amines were isobutylamine, piperidine, morpholine, piperazine, thiomorpholine, and dioxane. The latter two are not actually amines but are polar heterocycles, isostructural with morpholine and piperazine. These secondary organic compounds were purchased in their highest purity from Aldrich Chemical. The ratios of the various components run are shown in Table 1. The reactions were carried out in near 11.5 mL volumes using Parr 4745 stainless steel reactors loaded onto a home-built spit rotating at 43 rpm in a Blue M convection oven. The reactors use a Teflon cup to hold the reactants. Reactions were carried out at 170 °C. This particular zeolite product crystallized as aggregates of thin sheets[39] and as such the particles do not always nicely settle to the bottom of the reactor. This makes crystallization more difficult to assess by visual inspection alone. By sampling and using SEM analysis, the reaction can be considered complete when a preponderance of wavy, layerlike material is observed. An example is given in Figure 12. The solid contents of the reactor were then washed on glass frits with about a liter of water. The dried solids were then ready for characterization. In some instances, the recovered materials were subjected to an additional treatment to remove organic material located between the sheet layers, but possibly not in the pores themselves. In these instances, the dried solid was placed back in the same type of Parr reactor, immersed in DMF (10 mL), and this mixture heated for two days at 150 °C without stirring. The recovered material can be washed in a filter, as above.

**Characterization**: Solids, after washing and drying, were analyzed on a Siemens D-500 X-ray diffractometer. The electron microscopy was carried out on a Philips scanning electron microscope. TGA/MS analyses on the contents of organic material and water within the pores was carried out using a programmed ramp and heating to 700 °C. The instrumentation has been described previously by us.[40] Nitrogen micropore measurements were performed on a Micromiretics Model 2400 using calcined samples. Studies on the pore-filling by argon, using both static and dynamic methods, were performed by methods recently described by us.[41] $^{13}C$ MAS NMR spectroscopy was carried out on the samples as follows: $^{13}C$ MAS (magic angle spinning) NMR experiments were performed using a Bruker DSX 200 spectrometer. The probe was doubly tuned for $^{1}H$ and $^{13}C$ observation at frequencies of 200 and 50 MHz, respectively. A prepared sample was packed in a 7 mm $ZrO_2$ rotor and was spun at 4.0 kHz during the Bloch decay measurement. Delay time was adjusted to be long enough ($\approx$10 s) to get a fully relaxed $^{13}C$ NMR spectrum so that NMR quantitation should be valid. The number of transients was typically around 15000. The GC work to characterize decomposition products for the *N,N,N*-2-adamantammonium cations used in the SSZ-25 synthesis at 175 °C was performed by extracting neutral components into diethyl ether from the filtrate at the end of the zeolite synthesis reaction. These diethyl ether extracts were then injected (through a system with a splitter) onto a special column containing 4 wt% KOH and developed specifically for amine separation (Supelco). The adamantanol decomposition fragment was determined by co-elution of the pure compound to the same retention time.

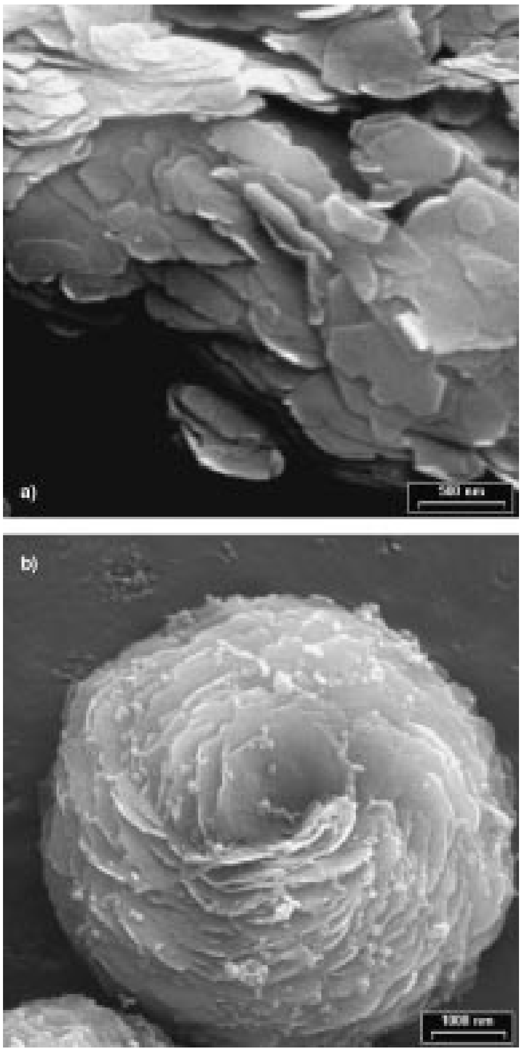

Figure 12. Scanning electron microscope (SEM) images of crystallized SSZ-25. a) The wavy surface is representative of our products in this study where two organic components are used and reactions are tumbled. b) Much longer range order for the placement of the layers is seen in the product from a static synthesis, using only the quaternary ammonium adamantane.

## Acknowledgements

We thank several individuals at Chevron Research and Technology Company for their contributions. LunTeh Yuen helped in some of the synthesis experiments. Dr. Chuck Kibby provided analyses by argon adsorption experiments. Dr. Ronald C. Medrud provided the XRD data. The late Robert A. van Nordstrand is thanked for his early interest in this problem and Dr. Cliff Detz and Dr. Dennis O'Rear are thanked for their enthusiastic support of the Chevron-Caltech collaboration in zeolite synthesis.

[1] R. Ravishankar, S. Tapas, R. Veda, H. S. Soni, S. Ganapathy, S. Sivasanker in *Zeolites and Related Microporous Materials: State of the Art 1994*, *Studies in Surface Science and Catalysis*, *Vol. 84* (Eds.: J. Weitkamp, H. G. Karge, H. Pfeifer, W. Holderich), Elsevier, Amsterdam, **1994**, p. 331.

[2] M. A. Camblor, C. Corell, A. Corma, M. J. Diaz-Cabanas, S. Nicolopoulos, J. M. Gonzalez-Calbet, M. Vallet-Regi, *Chem. Mater.* **1996**, *8*, 2415.

[3] S. L. Lawton, M. E. Leonowicz, R. D. Partridge, P. Chu, M. K. Rubin, *Microporous Mesoporous Mater.* **1998**, *23*, 109.

[4] A. Corma, *Microporous Mesoporous Mater.* **1998**, *21*, 487.

[5] S. Ernst in *Molecular Sieves 1*, *Science and Technology: Synthesis* (Eds.: H. G. Karge, J. Weitkamp), Springer, Heidelberg, **1998**, p. 65.

[6] S. I. Zones, Eur. Pat. Appl. 231 860, **1987**.

[7] L. Puppe, J. Weisser, DE 3 117 135, **1982**.

[8] M. K. Rubin, P. Chu, US 1 494 325, **1990**.

[9] R. Millini, G. Perego, W. O. Parker, G. Bellussi, L. Carluccio, *Microporous Mater.* **1995**, *4*, 221.

[10] M. E. Leonowicz, J. A. Lawton, S. L. Lawton, M. K. Rubin, *Science* **1994**, *264*, 1910.

[11] G. J. Kennedy, S. L. Lawton, A. S. Fung, M. K. Rubin, S. Steuernagel, *Catal. Today* **1999**, 385.

[12] A. Corma, V. Gonzales-Alfaro, A. V. Orchilles, *Appl. Catal. A* **1995**, *129*, 203.

[13] A. Corma, C. Corell, F. Llopis, A. Martinez, J. Perez-Pariente, *Appl. Catal. A* **1994**, *115*, 121.

[14] R. A. Innes, D. L. Holtermann, US 5 149 894, **1992**.

[15] D. N. Mazzone, C. R. Venkat, P. J. Lewis, B. P. Maerz in *Hydrocarbon Asia* (April issue) **1997**, p. 56.

[16] M. E. Davis, S. I. Zones, *Synthesis of Porous Materials* (Eds.: M. L. Occelli, H. Kessler), Marcel Dekker, New York, **1995**, p. 1.

[17] M. A. Camblor, M. J. Diaz-Cabanas, C. Corell, A. Corma, Spanish P9501553, **1995**.

[18] R. M. Barrer, *Hydrothermal Synthesis of Zeolites*, Academic Press, London, **1982**.

[19] S. I. Zones, R. A. Van Nordstrand, D. S. Santilli, D. M. Wilson, L-T Yuen, L. D. Scampavia in *Zeolites*, *Facts*, *Figures*, *and Future*, *Studies in Surface Science and Catalysis*, *Vol. 49A* (Eds.: P. A. Jacobs, R. A. van Santen), Elsevier, Amsterdam, **1989**, p. 299.

[20] M. A. Camblor, A. Corma, M. J. Diaz-Cabanas, C. Baerlocher, *J. Phys. Chem. B* **1998**, *102*, 44.

[21] S. I. Zones, Y. Nakagawa, PCT Patent Appl. WO 96/29284, **1996**.

[22] J. M. Nanne, M. F. M. Post, W. H. J. Stork, European Patent 12,473, **1979**.

[23] A. Corma, V. Fornes, S. Pergher, T. L. Maesen, J. Buglass, *Nature* **1998**, *396*, 353.

[24] A. Stewart, *Zeolites* **1989**, *9*, p. 140.

[25] S. Ernst, J. Weitkamp, *Chem. Ing. Tech.* **1991**, *63*, 748.

[26] D. E. W. Vaughn, G. C. Edwards, U.S. Patent 3,966, 883, **1976**.

[27] D. W. Breck in *Zeolite Molecular Sieves*, Kluwar Press, Florida, **1977**.

[28] P. Wagner, S. I. Zones, M. E. Davis, R. C. Medrud, *Angew. Chem.* **1999**, *111*, 1349; *Angew. Chem. Int. Ed.* **1999**, *38*, 1269.

[29] Y. Nakagawa, P. Wagner, G. S. Lee, R. C. Medrud, S. Elomari, M. E. Davis, S. I. Zones, *J. Am. Chem. Soc.* **2000**, *122*, 263.

[30] M. A. Camblor, L . A. Villaescusa, M. J. Diaz-Cabanas in *New Frontiers in Microporous Materials*, *Topics in Catalysis*, *Vol. 9 No. 1,2* (Eds.: S. I. Zones, C. T. Kresge), Balzer Scientific, Amsterdam, **1999**, p. 59.

[31] H. Gies, B. Marler in *Zeolites* **1992**, *12*, p. 42.

[32] G. Bellussi, G. Perego, A. Carati, U. Cornaro, V. Fattore in *Innovation in Zeolite Materials Science*, *Studies in Surface Science and Catalysis*, *37* (Eds.: P. J. Grobet, W. J. Mortier, E. F. Vansant, G. Schulz-Ekloff), Elsevier, Amsterdam, **1987**, p. 37.

[33] S. I. Zones, *Zeolites* **1989**, *9*, 409.

[34] B. M. Lowe, J. R. D. Nee, J. L. Casci, *Zeolites* **1994**, *14*, 610.

[35] M. E. Davis, R. F. Lobo, *Chem. Mater.* **1992**, *4*, 756.

[36] C. C. Freyhardt, M. Tsapatsis, R. F. Lobo, K. J. Balkus, M. E. Davis, *Nature* **1996**, *381*, 295.

[37] I. Mochida, S. Eguchi, M. Hironaka, S. Nagao, K. Sakanishi, D. Whitehurst, *Zeolites* **1997**, *18*, 142.

[38] S. I. Zones, D. L. Holtermann, R. A. Innes, T. A. Pecoraro, D. S. Santilli, J. N. Ziemer, U.S. Patent 5,591, 322, **1997**.

[39] I. Y. Chan, P. A. Labun, M. Pan, S. I. Zones, *Microporous Mater.* **1995**, *3*, 409.

[40] L-T Yuen, J. Geilfuss, S. I. Zones, *Microporous Mater.* **1997**, *12*, 229.

[41] C-Y. Chen, L. W. Finger, R. C. Medrud, C. L. Kibby, P. A. Crozier, I. Y. Chan, T. V. Harris, L. W. Beck, S. I. Zones, *Chem. Eur. J.* **1998**, *4*, 1312.

Received: January 28, 2000
Revised version: July 31, 2000 [F2265]